Density response to short-pulse excitation in gold

P. D. Ndione,[1] S. T. Weber,[1] B. Rethfeld,[1] and D. O. Gericke[2]

[1]*Department of Physics and Research Center OPTIMAS, Technische Universität Kaiserslautern, 67663 Kaiserslautern, Germany*

[2]*Centre for Fusion, Space and Astrophysics, Department of Physics, University of Warwick, Coventry CV4 7AL, United Kingdom*

Abstract

We investigate the dynamics of band occupation in gold after excitation with short laser pulses. Strong nonequilibrium distributions can be created by intra- and interband transitions driven by the absorption of photons with different wavelengths. First we shortly discuss how photons can be used as a probe and how electrons with non-Fermi distributions can be described. Then we focus on the relaxation stage where a temperature has been established but the occupation numbers in the different bands are not yet in equilibrium with this newly established, elevated temperature. We describe the relaxation towards a system with a common chemical potential with rate equations that can also include the energy transfer to the lattice or ions. Finally, we give an outlook on the optical response of the relaxing electron system to a probe pulse of radiation.

I. INTRODUCTION

Understanding the interaction of short pulses of laser light with matter is crucial for both fundamental science and applications. Moreover, it connects the physics of solids, warm dense matter and plasmas for stronger pulses as the material will undergo a series of phase transitions and relaxation stages during and after the excitation. Precise control of material processing is a premier example which requires a thorough knowledge of the energy deposition, energy loss channels and the relaxation processes driven by the laser [1, 2]. In particular, the use of lasers with femtosecond pulses has brought a new set of fundamental questions regarding the nature of the interaction process and the evolution of the material response [3]. Such short excitations drive a whole cascade of relaxation processes starting from the electron kinetics to the equilibration of electron and lattice temperatures with most of the associated relaxation rates being still under debate even for noble metals [4–7]. Moreover, the basic material properties, like the lattice stabilities and phonon modes, can change under laser irradiation [8, 9]. Such new transitions hold the promise of discovering new phases and metastable states and new chemical reaction pathways. Moreover, they present a standard way to create warm dense matter and dense plasmas states in the laboratory.

Ultra-short laser pulses are also a perfect tool to investigate the material response on very short time scales via its optical response at different wavelength [10]. One traditional way is to study Bragg scattering to investigate the lattice response in solids [11] and the creation of new phases [12, 13]. In the fluid and plasma phase, reflectivity and transmitivity measurements are a viable option that allow to reconstruct the dielectric function of the material after excitation [14–16]. For lower frequency probes using THz radiation, the wavefronts of the probe light can be determined which, again, provides the complex dielectric function [17]. For denser and more massive samples, x-ray Thomson scattering has been developed as a powerful optical probe to investigate the material properties [18, 19]. This method can also be applied to nonequilibrium situations [20–22] where it can yield important information on the relaxation processes initiated in the material.

For metals, the coupling of the laser field to the electrons is almost exclusively responsible for the absorption of the light and the subsequent material response is thus strongly connected to the electron relaxation [3, 23]. The electrons are driven far out of thermal

equilibrium both in their occupation numbers and the distribution functions. A few tens of femtoseconds after the initial excitation process electron-electron collisions lead to the thermalisation of the electron distribution [5, 24] if no further energy source, internal or external, is acting. Still, the temperatures of different bands as well as the occupation of the bands may not be in equilibrium as these processes usually require longer times [25]. On a picosecond time scale, the absorbed energy from the laser is shared with the lattice or the fluid ion component if melting occurs faster [5, 8, 24, 26]. This process is usually described within the two-temperature model keeping track of the electron and lattice/ion temperatures and links them by electron-ion coupling [27].

In this paper, we first report on optical probing under general nonequilibrium conditions and some basic concepts that allow to describe the electron relaxation within the framework of kinetic theory [28]. A special focus is here the important optical limit with negligible momentum transfer to the photon. In this case, it is sufficient to calculate the time-dependent occupation numbers in the bands instead of the full electron distribution function. Thus, the numerical effort is strongly reduced as we can employ rate equations for the occupation numbers and the fully kinetic description, e.g., with a Boltzmann-like equation is not needed any more. Within this rate equation approach, we first discuss the deviation of the initial energy into the two different bands available for optical excitation in gold. We then investigate the dynamic band occupation under different scenarios of laser excitation. Here, we find significant differences depending on the energy of the incoming photons. Finally, we give an outlook on how our results can be used to predict the optical response of laser-excited gold on time scales of a few picoseconds.

II. MODELS FOR THE OPTICAL PROPERTIES OF LASER-EXCITED MATTER

We consider the optical properties as an ideal tool to extract the material behaviour in nonequilibrium from observations. To inform experimental probing about the time-dependent electron properties, the dielectric function or the optical conductivity are the central quantities. In the optical, long wavelength limit $\vec{q} \to 0$, both complex quantities are connected via

$$\varepsilon(\omega) = \varepsilon_\infty + \frac{4i\pi}{\omega}\sigma(\omega)\,. \tag{1}$$

Here, ε_∞ denotes the static dielectric constant of the material under investigation. All other optical properties can be determined once the real and imaginary part of the dielectric function is calculated. For instance, we have for the reflectivity R of light with normal incidence

$$R = \frac{\left(1 - \sqrt{\frac{|\varepsilon| + \varepsilon_r}{2}}\right)^2 + \left(\sqrt{\frac{|\varepsilon| - \varepsilon_r}{2}}\right)^2}{\left(1 + \sqrt{\frac{|\varepsilon| + \varepsilon_r}{2}}\right)^2 + \left(\sqrt{\frac{|\varepsilon| - \varepsilon_r}{2}}\right)^2}, \tag{2}$$

where ε_r is the real part of the dielectric function and $|\varepsilon|$ its magnitude. Without absorption, the transmitivity then follows via $T = 1 - R$. However, similar relations can be also found for absorbing matter and other properties. Thus, we would have full access to the optical response of the material to any electromagnetic field once its dielectric function is known exactly. In equilibrium, this information might be obtained from *ab initio* simulations via the Kubo formula (see, e.g., Ref. 29). However, such an approach is illusive for matter far from equilibrium. Thus, we will need to develop approximate approaches for states that are driven or at states during the relaxation towards equilibrium.

One of the most applied approximation scheme for the dielectric function is the random phase approximation (RPA). Its standard form is valid for weakly interacting electrons within the conduction band (extensions for transitions between bands exist as well). For such systems, the dielectric function reads

$$\varepsilon^L(\vec{q}, \omega) = 1 - \frac{4\pi e^2}{\vec{q}^2} \chi^0(\vec{q}, \omega)\,. \tag{3}$$

Here, $\chi^0(\vec{q}, \omega)$ is the free-particle density response function (Lindhard function) and its prefactor is the Coulomb potential. This density response of ideal electrons to a perturbation with momentum $\vec{q}$ and energy $\hbar\omega$ is fully determined by the electron distribution function $f(E_{\vec{k}})$ as [30]

$$\chi^0(\vec{q}, \omega) = \frac{1}{V} \sum_{\vec{k},\sigma} \frac{f(E_{\vec{k}}) - f(E_{\vec{k}+\vec{q}})}{E_{\vec{k}+\vec{q}} - E_{\vec{k}} - \hbar\omega + i\eta}\,. \tag{4}$$

Here, the summation runs over all spins σ and momenta $\vec{k}$ in the conduction band, $f(E_{\vec{k}})$ denotes the time-dependent electron distribution and $E_{\vec{k}}$ denotes the dispersion relation in the band. For quasi-free electrons, we have for instance $E_{\vec{k}} = \hbar\vec{k}^2/2m^*$, where medium effects are condensed in the effective mass m^*. Within RPA, the parameter η is to be taken in the limit $\eta \to 0$ and insures the correct integration of the poles.

The random phase approximation above does not include any damping of the one-particle motion. Using a relaxation time ansatz, one may conclude that damping can be included by replacing the parameter η with a finite, real valued constant. However, such an approach would break basic conservation laws. An appropriate expression, that includes damping and conserves particle number, has been given by Mermin [31]

$$\varepsilon^M(\vec{q},\omega) = 1 + \frac{(1+i/\tau^D\omega)(\varepsilon^L(\vec{q},\omega+i/\tau^D)-1)}{1+(i\omega/\tau^D)(\varepsilon^L(\vec{q},\omega+i/\tau^D)-1)/(\varepsilon^L(\vec{q},0)-1)}\,, \tag{5}$$

were ε^L denotes Lindhard dielectric function (3) and τ^D is the damping constant or inverse of the collision frequency. This approach is particular useful if both a finite momentum transfer due to the excitation or probing and significant damping due to collisions occurs.

For many experiments, the dielectric function is only needed in the optical limit $\vec{q} \to 0$ as the photon transfers no momentum in normal incidence. In this case, a significant simplification arises as we also have $\hbar\omega \gg \left|E_{\vec{k}} - E_{\vec{k}\pm\vec{q}}\right|$. Thus, the real part of the dielectric function can be written as

$$\varepsilon_r^L(0,\omega) = 1 - \frac{4\pi e^2}{m^*\omega^2}\int dE_{\vec{k}}\; f(E_{\vec{k}})\; D(E_{\vec{k}})\,, \tag{6}$$

where $D(E_{\vec{k}})$ is density of states (DOS) in the material of interest. The integral is simply the occupation of the conduction band. Thus, we don't require knowledge of the full distribution function but only of the density of electrons in the relevant band to describe the optical response in the long wavelength limit.

When we include damping in the description, the Mermin expression can be condensed into the Drude formula [32]

$$\varepsilon^D(\omega) = \varepsilon_\infty - \frac{n\; e^2}{m^*\,\varepsilon_0}\;\frac{1}{\omega\,(\omega+i/\tau^D)}\,. \tag{7}$$

Again, ε_∞ labels the static dielectric constant which differs significantly from unity in noble metals. The electron density n is to be taken from the optically active bands only. As for the RPA in the optical limit, the Drude approach does not require the time-dependent distribution function but only the evolution of the occupation number in the conduction band which poses a significant simplification of any theoretical approach. Clearly, the Drude formula approaches the optical limit of the Lindhard dielectric function for $\omega\tau^D \gg 1$.

III. MODELS FOR THE DENSITY EVOLUTION IN GOLD

We consider gold as a prototype of a metal with a complex band structure. For optical excitations, the active band is the *sp*-band which might be seen as acting similarly to the free electrons in a hot plasma. The *d*-band acts as a reservoir of electrons that can be excited to the *sp*-band by the laser similarly to bound states in a plasma. As a result of the excitation, we will have a hot electron ensemble in the *sp*-band that contains more than the usual one electron per atom for $T = 0$. The subsequent relaxation will then establish a Fermi distribution of electrons over both bands that is defined by a temperature and a chemical potential common to both bands. In the following, we will present two approaches that describe the relaxation process towards this well-defined equilibrium state.

As we have shown in the previous section, we need the full electron distribution function for the description of the optical properties of the excited system within the Lindhard (3) and the Mermin (5) approach. This distribution may be obtained as a solution of an appropriate kinetic equation [28]. An example is the Boltzmann equation which, in the homogeneous case without external fields, can be solved together with a similar equation for the phonon/ion occupation [5, 24]

$$\frac{\partial f(E_{\vec{k}},t)}{\partial t} = \Gamma_{\text{el-el}} + \Gamma_{\text{el-ph}} + \Gamma_{\text{absorp}}\,, \tag{8}$$

$$\frac{\partial g(E_{\vec{q}},t)}{\partial t} = \Gamma_{\text{ph-el}}\,, \tag{9}$$

where $g(E_{\vec{q}},t)$ represents the phonons' distribution function in energy space and with dispersion $E = E(\vec{q})$. Taking the density of states as an input, the system above can be solved numerically by treating both *sp*- and *d*-electrons as an effective common band of isotropic electrons. Refs. 24 and 33 show results for gold and copper highlighting the need for an accurate DOS.

Direct solutions of the Boltzmann equations are usually very complex and numerically expensive. Moreover, the description of optical properties in the long wavelength limit does not require the full energy-resolved distribution. Hence, we aim to use a simpler approach based on rate equations. Since the electron thermalization has been found to occur on a timescale of a few tens of femtoseconds [24, 28], the full kinetics of the electron relaxation is not much of importance on timescales of several tens of femtoseconds to picoseconds. Here, we can safely assume a Fermi distribution for the electrons in each band. Furthermore, a

common temperature between the bands is also quickly established. However, the occupation number of each band can still be out of equilibrium with respect to both the common temperature and the occupations of the other bands. Similar situations have also been considered for excited electrons in semiconductors [34, 35]. For bismuth, such approach of a so-called constrained density, has also been applied [36, 37] within a density functional theory calculation.

To determine the evolution of the band occupation, we set up a system of rate equations containing all transitions between the bands involved and taking into account the restrictions and simplifications mentioned above. For gold excited by optical light, we consider two bands: one valence (d) and one conduction band (sp). The DOS for gold shows that both bands overlap but the energy of the photons must be sufficient to excite significant numbers of electrons beyond the Fermi energy. All electrons are considered to have the same temperature which is set by the total energy deposited by the laser. Moreover, our rate equations need to allow for heating of the band by intraband transitions as well as d to sp transfer. Due to energy conservation and the known Fermi distribution of the equilibrium case, we also know the final band occupation after the relaxation. Thus, we can use a simple relaxation time ansatz to determine the rate of electron transfer between the bands. This relaxation time is here a free parameter of the calculation. In summary, our set of rate equations for the evolution of the band occupation reads

$$\frac{dn_{sp}}{dt} = \frac{\alpha_{\text{inter}}}{\hbar\omega_L} I_L - \frac{1}{\tau_{\text{relax}}} \left[n_{sp} - n_{sp}^{eq}(T_e) \right] = -\frac{dn_d}{dt} \,, \tag{10}$$

$$C_e \frac{dT_e}{dt} = \left[\alpha_{\text{intra}} + \alpha_{\text{inter}} \right] I_L - g_{ei}(T_e) \, \left[T_e - T_i \right] \,, \tag{11}$$

$$C_i \frac{dT_i}{dt} = g_{ei}(T_e) \, \left[T_e - T_i \right] \,. \tag{12}$$

The first term in Eq. (10) describes the increase of the electron density in the conduction (sp) band of gold due to excitation of $5d$ electrons by a laser with intensity I_L. The number of absorbed photons and thus the density of excited electrons is determined by the absorbed energy and the energy of one photon $\hbar\omega_L$. In our rate equations, it is governed by the interband absorption coefficient α_{inter} and the photon energy $\hbar\omega_L$. The second term describes the effective transfer of d-electrons to the sp-band or sp-electrons to the d-band until the equilibrium density $n_{sp}^{eq}(T_e)$ is reached. Again, the latter is uniquely defined by the electron temperature T_e (see also Ref. 38). The rate of electron transfer is characterised by the relaxation time τ_{relax}. The energy equation (11) determines the time-dependent electron

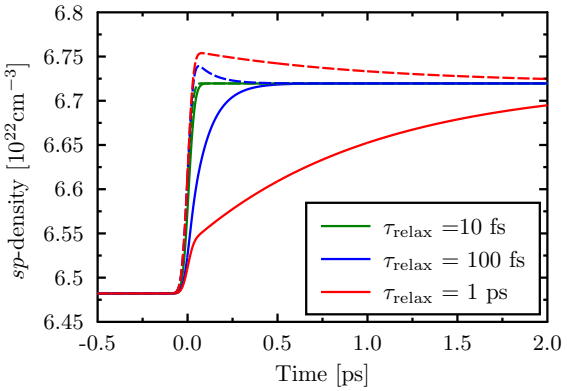

FIG. 1. Time-dependent *sp*-density in gold as calculated with the rate equations (10) for a 60 fs laser pulse with a photon energy of 3.1 eV. The laser induces excitation of *d* electrons to the *sp* band that has an initial density of $6.48 \times 10^{22}\,\mathrm{cm}^{-3}$. The system then relaxes to an equilibrium density of $n_{sp}^{eq}(T_e) = 6.72 \times 10^{22}\,\mathrm{cm}^{-3}$. Solid and dashed lines correspond to 10% and 50% of the total energy being absorbed by *d*-electrons, respectively

temperature which rises during the laser pulse and then stays constant if no other energy source or sink is considered.

Of course, the rate equations (10) are coupled with the conservation of total electron density: $n_{\mathrm{tot}} = n_{sp} + n_d$ which determines the *d*-band occupation. Moreover, we coupled the equations for the electron energy with an equation describing the phonons or ions as an energy sink (12), thus, reducing the electron temperature on the time scale of electron-phonon or electron-ion energy relaxation. The coupling parameter used is temperature-dependent and taken from Ref. 39. As input, our rate equations require a split of the excitation energy to a part that initiates a transfer of *d*-electrons to the conduction band $\alpha_{\mathrm{inter}} I_L$ and a part that only heats the conduction band $\alpha_{\mathrm{intra}} I_L$, the relaxation time towards an equilibrium band occupation, the electron-phonon/ion energy transfer rate and the density of states of the material to be considered.

IV. RESULTS AND DISCUSSION

Now we take laser-excited gold as an example to discuss the dynamics of the band occupation described by the rate equations (10). In the first example, we split the laser energy

arbitrarily between the d-band and sp-band electrons to discuss the general behaviour of the relaxation process. Fig. 1 displays results for the time-dependent density in the conduction band of gold employing a range of different relaxation times. As we consider only two active bands, changes to the d-band density are just the inverse to any change in the sp-density. In all cases, we see first a rather sharp rise of the conduction band occupation due to photons being absorbed in the d-band and being transferred into the conduction band. This increase is later overlaid with a further increase or decrease of sp-density due to the relaxation process towards the equilibrium occupation.

In cases, where only 10% of the laser energy is absorbed by electrons in the d-band and 90% simply heats the sp-band, we find a significant transfer of further electrons into the conduction band until the hot temperature and the occupation are in equilibrium. Of course, the time scale of this process is set by the relaxation time. When the energy input is split equally between d- and sp-electrons, we have the opposite case: here, the temperature cannot sustain the high sp-density created by the laser and the relaxation after the excitation slightly reduces the conduction band energy. This fact demonstrates that a good description of the different absorption channels, in particular the ratio of energies deposited into the d- and sp-band, is essential for predictions of the density response of many metals having a complex band structure such as gold or copper. We want to point out that all cases have the same final energy density and, thus, the same final temperature is reached although the relaxation process is not finished for the case with largest relaxation time τ_{relax} during time shown in the figure.

For further studies, we need a more realistic description of the laser absorption into the two different bands. Here, we consider a total absorption coefficient as determined previously [40, 41]. The total absorption is split into a part that promotes d-band electrons into the sp-band and one part that only heats the sp-band via intraband transitions. Thus, we define the absorption coefficient of interband transfers via

$$\alpha_{\mathrm{inter}} = \alpha_{\mathrm{total}} \, \frac{\Omega_d}{\Omega_d + \Omega_{sp}} \,, \tag{13}$$

where Ω_d and Ω_{sp} are the numbers of electrons that can absorb photons and are in the d- and sp-band, respectively. As the d-band will stay almost full, intraband absorption in the d-band will be highly restricted by the Pauli principle. Thus, we consider that all photons being absorbed by d-electrons initiate the transfer of these electron into the conduction band.

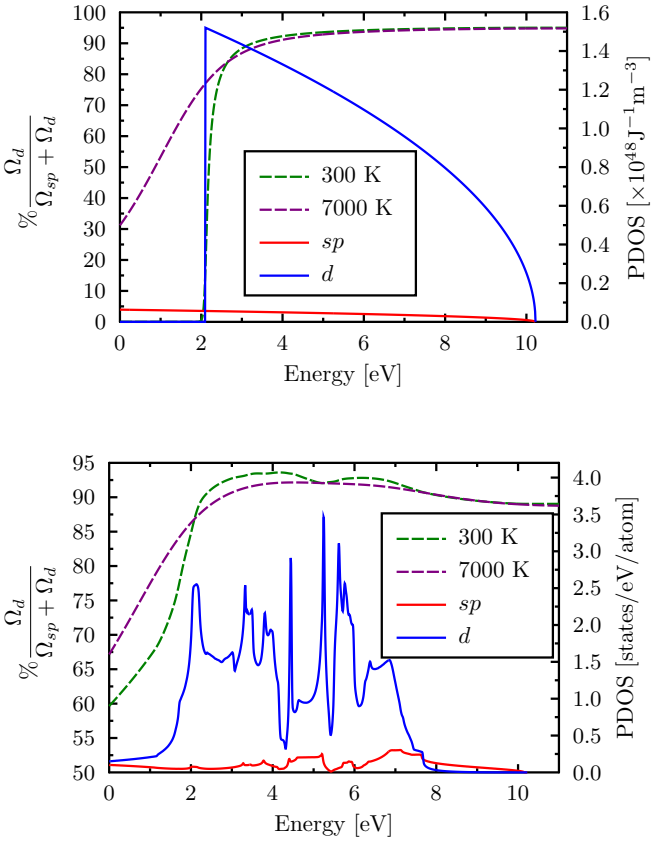

FIG. 2. Ratio of the number of photons absorbed into the d-band, thus initiating a d to sp transfer, to the total number of absorbed photons for two temperatures. The panel on the left assumes a simplified model of two parabolic bands; the panel on the right considers the density of states as calculated from density functional theory [42]. Both panels show the inverted DOS that was employed in the calculation.

We also assume that both d- and sp-electrons absorb a photon with the same probability. Moreover, the transfer is only possible when the final state of the transferred electron was available. Thus, the fraction Ω_j is proportional to the density of j-electrons and the Pauli-blocking factor $[1-f]$ for the states with an energy $E+\hbar\omega$

$$\Omega_j = \int dE\, D_j(E) f_j(E,t) \left[1 - f_j(E+\hbar\omega, t)\right], \tag{14}$$

where $D_j(E)$ is the partial density of states for the band considered.

Figure 2 shows the results for the fraction of photons to be absorbed by d-band electrons and, thus, increasing the density in the conduction band as a function of photon energy.

For low temperatures, this clearly follows the number of d-band electrons in states where this energy transfer is not prohibited by the Pauli blocking. Thus, mainly electrons within a photon energy ($\hbar\omega_L$) below the Fermi energy can contribute to absorption. Their number strongly depends on the density of states. To highlight the number of accessible electrons, we have also included the inverted density of states in the figure. For higher temperatures, the Pauli principle does not act as severe as more and more states become available as final states for the transition. Thus, we find a much higher Ω_d even for small photon energies. Higher photon energies also transfer more electrons into states far beyond the Fermi energy. Thus, d-band absorption is much higher for larger photon energies. Indeed, the fraction of energy absorbed by d-band electrons becomes almost independent of the temperature for photon energies above 3 eV.

For small photon energies the ratio of d-band to sp-band absorption is highly sensitive to the form of the density of states. To highlight this fact, we show results employing a realistic DOS determined by density functional theory [42] in the right panel of Fig. 2 and data using a simple DOS consisting of two parabolic bands (one finite to mimic the d-band and one open to describe sp-electrons) in the left panel. The largest deviations are found for cold electrons and at small photon energies. As the simple model has only d-states

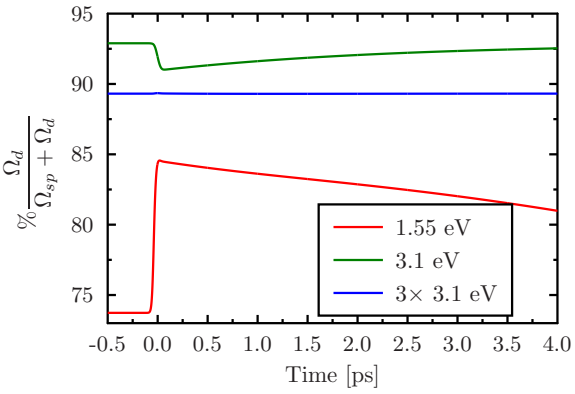

FIG. 3. Evolution of the fraction of the number of photons absorbed by the d-band for three different photon energies. The laser excitation is 60 fs long and has its peak at $t = 0$. The graphs show the relative absorption by the d-band for any additional photon that would reach the system at time t, not only the real absorbed laser energy around $t = 0$.

$> 2.1\,\mathrm{eV}$ below from the Fermi energy, no d-band absorption is possible for photon energies below 2.1 eV. For slightly larger photon energies, the absorption of the d-band then rises sharply. This behaviour is not visible in the results using the more realistic density of states. Here, the d-band has a small but finite contribution for all states up to the Fermi energy and beyond. Thus, absorption by d-electrons is always possible even for low temperatures as $T = 300\,\mathrm{K}$. Accordingly, we find a significant fraction of photons promoting additional electrons into the sp-band even for very small photon energies. The fraction Ω_d also rises with temperature but not as strongly as for the simple model used in the left panel.

Of course, any real laser pulse will interact with a system having a very dynamic response starting at a low temperature followed by a sharp rise. Fig. 3 shows the evolution of absorption of d-electrons for a realistic heating scenario. Here, a short laser pulse heats the system and initiates a transfer of d-electrons into the sp-band followed by a density response described below. The largest changes in the d-band absorption occur during the laser pulse. At this time, final states unavailable before become free due to the excitation and the number of valence electrons that can absorb is decreasing as more and more electrons are transferred into the conduction band. Clearly, the first process is more important for small photon energies (1.55 eV) as most accessible states are still occupied for small temperatures but become partially free due to the electron excitation by the laser pulse. Higher photon energies (3.1 eV) can promote many d-electrons beyond the Fermi energy and thus are only slightly restricted by the $[1 - f]$-term in Eq. (14). Here, the reduction of d-band electrons is more important and, accordingly, the part of d-band absorption decrease during the laser pulse.

The long time behaviour of the absorption is more academic and related to the effect of a second heating pulse. It mainly reflects the relaxation of band occupation after the initial heating as well as electron transfer processes. As different photon energies result in a different relaxation behaviour as will be discussed below, the absorption of additional photons also shows a different trend with time.

We now inspect again our results for the density evolution. For a more realistic split of the laser energy beween d- and sp-bands, we employ the procedure based on the density of states from DFT calculations as presented above. Fig. 4 shows results for the relaxation process in gold driven by a 60 fs long laser pulse with different photon energies. To allow for an easy comparison, all cases have the same absorbed energy, and thus induced electron

temperature. Therefore, all systems relax towards the same final *sp*-density. Moreover, we consider the same *sp* to *d* relaxation time of $\tau_{\mathrm{relax}} = 600\,\mathrm{fs}$ in all cases, a value consistent with the thermalization time of nonthermal electrons in gold [43, 44].

The sharp rise of conduction band density around $t = 0$ is created by the direct transfer of *d*-electrons into the conduction band by the laser radiation. As the absorbed energy is equal in all calculations shown, there are many more photons absorbed for cases with low photon energy (cases in the left panel) as compared to higher photon energies (right). Accordingly, the initial rise in the number of conduction band electrons is stronger in these cases. For the three cases in the left panel, this fact results in an over-population of the *sp*-band which

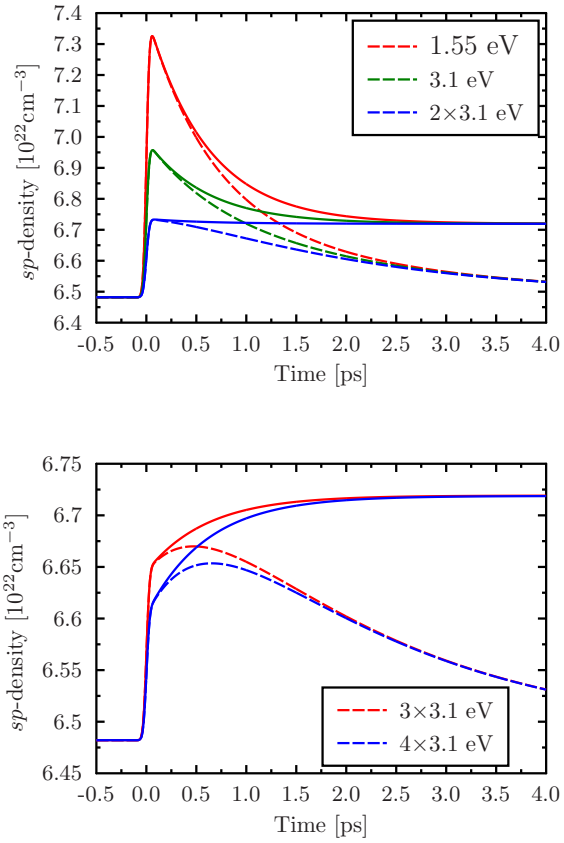

FIG. 4. Time-dependent *sp*-density in gold as calculated using the rate equations (10) for a 60 fs laser pulse with different photon energies. The laser induces excitation of *d* electrons to the *sp* band that has an initial density of $6.48 \times 10^{22}\,\mathrm{cm}^{-3}$. Full lines consider the electron system only while dashed lines include electron cooling via a coupling with the phonon system. All cases have the same absorbed energy of $1.35 \times 10^5\,\mathrm{J/kg}$ ($2.6 \times 10^9\,\mathrm{J/m}^3$).

is then reduced in the subsequent relaxation. In the two cases with high photon energies drawn in the right panel of Fig. 4, much fewer photon are absorbed and, thus, much fewer d-band electrons are transferred to the sp-band. However, the common temperature is the same after the laser pulse due to the larger energy input per photon. Accordingly, the same final density is reached in equilibrium which results in a further increase of the conduction band density during the relaxation phase. This qualitatively different behaviour with photon energy is relatively independent from the free parameters in the model and should create a clear observable for experiments independent of the probe used.

Figure 4 contains also results where the energy transfer between the electrons and the lattice / phonons is taken into account. Here, the energy transfer is modelled by a temperature-dependent electron-phonon coupling parameter [39]. As the phonons act as an energy sink, the electron temperature decreases during the relaxation and, in turn, the conduction band density is reduced as well. As this process runs on a time scale of a few picoseconds, it should also be observable experimentally. The most interesting signature is found for the high photon energies. Here, the electron-phonon interaction reverses the secondary increase of the conduction band density after roughly a picosecond while for lower photon energies it simply enhances the already existing trend.

With the results for the density evolution, we are now able to calculate the optical properties for the electron system in nonequilibrium. Here, we present only preliminary results based on the Drude model (7). This means our results consider only intraband contributions from the sp-electrons while d-electrons contribute only negligible due to their heavy effective mass. Moreover, interband transitions between the bands are not included. Usually, interband contributions are considered to be small for small probe wavelength. However, it is known that they increase strongly with temperature. In our case, we expect also large contributions from interband transitions as the nonequilibrium situations considered exhibit many holes at energies below the Fermi edge.

Still, the Drude description already yields some interesting behaviour: depending on the model for the damping parameter in the Drude formula, the real part of the dielectric function either increases or decreases at the time of the excitation while the imaginary part always increases. This interesting behaviour of the real part is driven by the strong increase of the collision frequency due to collision of sp-electrons with electrons from the d-band as predicted in Ref. 38. Collisions within the sp-band are found to give only all

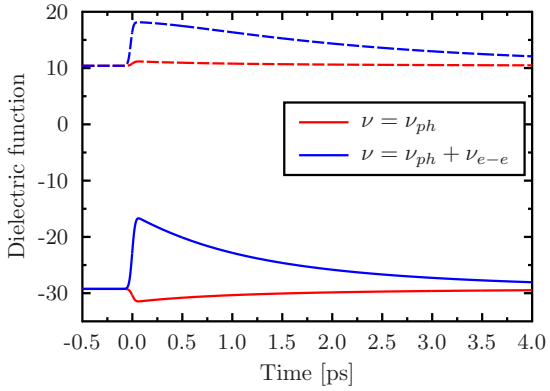

FIG. 5. Evolution of the dielectric function as calculated with the Drude form (7) for a relaxing electron system in gold. The dashed line label the imaginary part and the full lines the real part of the dielectric function. Both are plotted for a probe energy of 1.55 eV. The underlying density relaxation is the same as shown in Fig. 4 for an excitation energy of 3.1 eV including electron-phonon interaction (dashed green line). The Drude damping rate is calculated in two ways: either only electron-phonon interactions are considered or electron-phonon as well as electron-electron interactions are included as described in Ref. 38. Note that the quantity plotted is only the intraband contribution to the dielectric function and strong interband contributions are expected here as well, in particular, for times with strong nonequilibrium occupation of the bands.

small contribution while the *d*-electrons can act as a independent collision partner for the *sp*-electrons which determine the optical properties. As Pauli-blocking plays a major role before heating but only a minor role for the elevated temperatures after the excitation, there is a strong increase in the collision frequencies with *d*-electrons. This increase of collision frequency fully overrules the calculated increase in the *sp*-band density, that is, the increase in plasma frequency of the conduction band. Although this results seems to contradict experimental data [15, 16], one must keep in mind that the interband contribution may change this prediction even on the qualitative level.

V. CONCLUSION

We have developed a model to describe the electron relaxation in metals after strong excitation with short laser pulses. The model is based on rate equations describing the occupation numbers of the *d*- and *sp*-band in gold. Being designed to model the intermediate relaxation stage of a few picoseconds, we consider the electron energy relaxation to be finished and a Fermi distribution to be established. Thus, we can define a temperature for the electrons. This temperature can also be coupled to a lattice temperature to include electron-phonon interactions. Based on the density of states, we have also developed a model that describes the split of laser energy into the different absorption channels. While absorption by *d*-electrons promotes these electrons into free states of the *sp*-band, photons being absorbed by *sp*-electrons only increase the temperature. The predictions of the rate equations for the conduction band density show an interesting behaviour: small photon energies result in a conduction band density that is higher than its equilibrium value while photons with several eV or more produce conduction band densities that are too low for the energy content of the electron system. Thus, the subsequent relaxation reduces or increase the number of electrons in the conduction band, respectively. The resulting *sp*-band densities can now serve as a basis to calculate the optical properties of laser-excited gold. However, easy models neglect the interband contributions and can be thus in contradiction with experimental results.

VI. ACKNOWLEDGEMENT

Financial support from the Deutsche Forschungsgemeinschaft through the Heisenberg grant RE1141-15 and from the Carl-Zeiss Stiftung is gratefully acknowledged. We appreciate the Allianz für Hochleistungsrechnen Rheinland-Pfalz for providing computing resources through project LAINEL on the Elwetritsch high performance computing cluster.

---

[1] B. N. Chichkov, C. Momma, S. Nolte, F. von Alvensleben and A. Tünnermann, Appl. Phys. A **63**, 109 (1996).

[2] D. Bäuerle, *Laser Processing and Chemistry* (Springer, Berlin, Heidelberg, 2011).

[3] B. Rethfeld, D. S. Ivanov, M. E. Garcia and S. I. Anisimov, J. Phys. D: Appl. Phys. **50**, 193001 (2017).

[4] D. O. Gericke, S. Kosse, M. Schlanges and M. Bonitz, Phys. Rev. B **59** 10639 (1999).

[5] B. Rethfeld, A. Kaiser, M. Vicanek and G. Simon, Phys. Rev. B **65**, 214303 (2002).

[6] N. Medvedev, U. Zastrau, E. Förster, D. O. Gericke and B. Rethfeld, Phys. Rev. Lett. **107**, 165003 (2011).

[7] T. G. White *et al.*, Phys. Rev. B **90**, 014305 (2014).

[8] V. Recoules *et al.*, Phys. Rev. Lett. **96**, 055503 (2006).

[9] R. Ernstorfer, M. Harb, C. T. Hebeisen, G. Sciaini, T. Dartigalongue, and R. J. D. Miller, Science **323**, 1033 (2009).

[10] A. A. Yurkevich, S. I. Ashitkov and M. B. Agranat, Phys. Plasmas **24**, 113106 (2017).

[11] M. Nicoul *et al.*, Appl. Phys. Lett. **98**, 191902 (2011).

[12] D. Kraus *et al.*, Nature Commun. **7**, 10970 (2016).

[13] D. Kraus *et al.*, Nature Astrophysics **1**, 606 (2017).

[14] P. Celliers, A. Ng, G. Xu, and A. Forsman, Phys. Rev. Lett. **68**, 2305 (1992).

[15] T. Ao *et al.*, Phys. Rev. Lett. **96**, 055001 (2006).

[16] Z. Chen *et al.*, Phys. Rev. Lett. **110**, 135001 (2013).

[17] T. Kampfrath, D. O. Gericke, L. Perfetti, P. Tegeder, M. Wolf and C. Frischkorn, Phys. Rev. E **76**, 066401 (2007).

[18] S. H. Glenzer and R. Redmer, Rev. Mod. Phys. **81** 1625 (2009).

[19] L. B. Fletcher *et al.*, Nature Photon. **9**, 274 (2015).

[20] G. Gregori, S. H. Glenzer and O. L. Landen, Phys. Rev. E **74**, 026402 (2006).

[21] D. A. Chapman and D. O. Gericke, Phys. Rev. Lett. **107**, 165004 (2011).

[22] U. Zastrau *et al.*, Phys. Rev. Lett. **112**, 105002 (2014).

[23] V. Schmidt, W. Husinsky, and G. Betz, Phys. Rev. Lett. **85**, 3516 (2000).

[24] B. Y. Mueller and B. Rethfeld, Phys. Rev. B **87**, 035139 (2013).

[25] S. T. Weber and B. Rethfeld, arXiv preprint: 1801.06560 (2018).

[26] J. Vorberger, D. O. Gericke, Th. Bornath, and M. Schlanges, Phys. Rev. E **81**, 046404 (2010).

[27] S. I. Anisimov, B. L. Kapeliovich and T. L. Perel'man, Sov. Phys. JETP **39**, 375 (1974).

[28] M. Bonitz, *Quantum Kinetic Theory* (Teubner, Stuttgart/Leipzig, 1998).

[29] B. Holst *et al.*, Phys. Rev. B **90**, 035121 (2014).

[30] J. Lindhard, Mat. Fys. Medd. **28**, 8 (1954).

[31] N. D. Mermin, Phys. Rev. B **1**, 2362 (1970).

[32] P. Drude, Annalen der Physik **306**(3), 566 (1900).

[33] S. T. Weber and B. Rethfeld, Appl. Surf. Sci. **417**, 64 (2017).

[34] H. M. van Driel, Phys. Rev. B **35**, 8166 (1987).

[35] A. Rämer, O. Osmani, and B. Rethfeld, J. Appl. Phys. **116**, 053508 (2014).

[36] É. D. Murray, D. M. Fritz, J. K. Wahlstrand, S. Fahy and D. A. Reis, Phys. Rev. B **72**, 060301(R) (2005).

[37] É. D. Murray, S. Fahy, D. Prendergast, T. Ogitsu, D. M. Fritz and D. A. Reis, Phys. Rev. B **75**, 184301 (2007).

[38] C. Fourment *et al.*, Phys. Rev. B **89**, 161110 (2014).

[39] Z. Lin, L. V. Zhigilei and V. Celli, Phys. Rev. B **77**, 075133 (2008).

[40] P. B. Johnson and R. W. Christy, Phys. Rev. B **6**, 4370 (1972).

[41] W. S. M. Werner, K. Glantschnig and C. Ambrosch-Draxl, J. Phys. Chem. Ref. Data **38**, 1013 (2009).

[42] J. K. Dewhurst *et al.*, *The elk FP-LAPW Code* (http://elk.sourceforge.net).

[43] W. S. Fann, R. Storz, H. W. K. Tom and J. Bokor, Phys. Rev. Lett. **68**, 2834 (1992).

[44] C.-K. Sun, F. Vallée, L. Acioli, E. P. Ippen, and J. G. Fujimoto, Phys. Rev. B **48**, 12365(R) (1993).